Characterization of Imaging Phone Cameras Using Minimum Description Length Principle

ADRIAN BURIAN[1], AKI HAPPONEN[2], MIHAELA CIRLUGEA[3]
[1] Devices Research and Development
Nokia
Visiokatu 1, 33720, Tampere
FINLAND
adrian.burian@nokia.com
[2] Devices Research and Development
Nokia
Elektroniikkatie 10, Oulu
FINLAND
aki.p.happonen@nokia.com
[3]Bases of Electronics Department
Technical University of Cluj-Napoca
Baritiu 26-28
ROMANIA
mihaela.cirlugea@bel.utcluj.ro

Abstract: - In this paper, a new Minimum Description Length (MDL) approach for the characterization of a mobile phone's color camera is presented. The use of high-order polynomials, Fourier sine series, and artificial neural networks (ANN) for solving this problem are compared and contrasted. The MDL formalism is used for determining the stochastic complexity of polynomial and Fourier sine models for the characterization of a Nokia N93 mobile phone camera. A quantitative evaluation of their performances, as well as for using an ANN, is provided.

Key-Words: - Minimum Description Length, High-Order Polynomial, Artificial Neural Network, Imaging Mobile Phone.

1 Introduction

Digital cameras are becoming increasingly important image acquisition tools to realize image and color processing. The accurate handling of the color characteristics of the obtained images is a difficult task, due to the fact that the *RGB* signals generated by a digital camera are device-dependent. Different digital cameras will produce different *RGB* responses for the same captured scene. Furthermore, while digital cameras bring simplicity in handling image capture, satisfying customer expectations is difficult as well. This is due to the fact that a camera captures the physical values of the light, while human observers perceive the result of processing of their visual systems.

The proliferation of camera phone devices in the consumer market has led to an increased need to transfer images among different storing/ manipulating/displaying mediums without loss of color fidelity [1]. Furthermore, the picture quality of camera phones is improving substantially enough that it is expected that these phones will begin to replace the low-end digital cameras [2]. The quality in even low-end camera phones will be enough to compete with low-end digital cameras. Already it is considered that, e.g., the two mega-pixels Nokia N90 with Carl Zeiss lens is a digital camera replacement. We must also specify that this is high-end phone, more costly than a high-end digital camera with five mega-pixels; so it is generally considered that the high-end market for digital cameras is safe.

We can consider that the images captured by a camera are depending mainly on three factors: the characteristics of the used camera, the illumination of the captured image, and on the actual color content of the scene. Since the camera is an integral part of the resulting image, research into image understanding normally requires a camera model. The most common use of camera characterization is to predict camera responses, given an input energy spectral distribution. This has applications in the development and practical realization of color-related image processing algorithms, such as computational color constancy algorithms. A common solution to obtain high-fidelity cross-media color reproduction is to characterize each device in terms of CIE tri-stimulus values [3, 10]. Using appropriate characterization procedures, it is possible to convert the camera *RGB* values to CIE *XYZ* values, and then to convert back the *XYZ* values to *RGB* ones on another medium, e.g., a monitor.

Before a capture can be shown on the display of a camera phone, the captured image data must first be processed. The processing sequence, or the reconstruction chain, contains functions to reconstruct the image from the sensor's data, to adjust the color of the image, to attenuate noise, to correct the geometrical distortions, and to adjust the sharpness of the image [4, 17, 18].

The quality of the final picture depends not only on the optical elements (lenses) and the imaging sensor, but also on the algorithms used in the reconstruction chain. The challenge for research is to develop processing methods that improve the image but are not too complicated for the phone engine to execute in real time.

In this paper, the MDL formalism will be used to compare the characterization of the digital camera of a Nokia N93 mobile phone, using polynomial transforms and Fourier sine transforms. We mention here that the MDL formalism was previously used in color processing for spatial segmentation of color images [3, 6, 9]. In addition, ANN are used and compared with the previous two approaches for camera characterization. In [6] the Levenberg-Marquardt (LM) optimization method was used for training a fully connected multi-layer perceptron network to derive mappings between the camera responses and tri-stimulus values. An Agfa digital StudioCam camera, a three-chip CCD device with 8-bit resolution for each channel and 4500 × 3648 pixel spatial resolution was used. The ANN contained three input units to receive the camera responses, three output units to output the tri-stimulus values and a single hidden layer. The number of units in the hidden layer was varied to be 3, 5, 10, 18, 27 or 40. The conclusion from [7] was that the optimum hidden layer has 18 units, and the obtained neural network has almost identical results with the more traditional technique of polynomial transforms. We considered that adding also neural networks to our study can be of interest; this is because for high-end cameras the camera responses exhibit an approximately linear relationship with the mean reflectance, or *Y* tri-stimulus value of the grey sample, while for low-end cameras this relationship is nonlinear. Our purpose in the case of ANN solution is again to obtain the smallest complexity, so we decided to use the method from [6] for training. This training method uses MDL as stopping criterion in order to avoid over-fitting and has feed-forward neural network architecture with a single hidden layer.

2 Characterization of Cameras

For the characterization of cameras, linear transforms are considered fundamental [5, 19, 20]. The camera characterization is the relationship between device coordinates (*RGB*) and some-device independent color space, such as CIE *XYZ*.

The polynomial approach appears to be a common method for obtaining the *XYZ* tri-stimulus values. This approach was also used in [8] for comparing a high-end digital camera with a low-end digital camera, in terms of accuracy of colorimetric characterization and “What You See Is What You Get" color texture simulation. Their conclusion was that the high-end digital camera clearly outperformed the low-end digital camera used in tests, in terms of texture simulation. The high-end camera produced mostly acceptable and good matches while the low-end camera produced mostly bad matches. We can also drawn the conclusion that polynomial transforms do not have good performances for low-end cameras, and we consider this to be in connection with their stronger nonlinear characteristics when compared to high-end cameras.

The most common and efficient method for characterizing a digital camera is to use a chart containing a set of colors of known tri-stimulus values. These charts include neutral patches that may be used to linearize the camera *RGB* responses, and colored patches that may be used for camera characterization to CIE *XYZ* values.

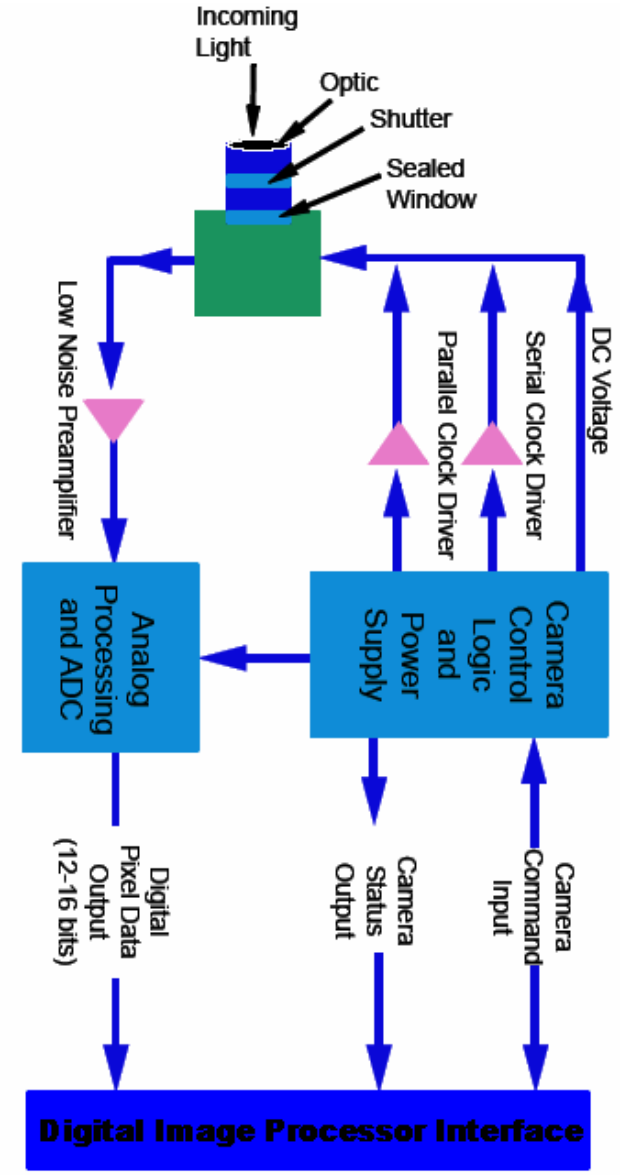

Fig. 1. Typical CMOS Camera Configuration

2.1 Image Formation in Color CMOS Cameras

Over the past years, there has been a growing interest in digital cameras based on CMOS (Complementary Metal Oxide Semiconductor) image sensors [9]. CMOS imager technology creates the opportunity for low-power low-cost highly integrated imaging systems, which is of great importance, for example, for wireless applications. A typical CMOS camera configuration is illustrated in Fig. 1.

A significant place in CMOS image formation is occupied by digital signal processing algorithms. These algorithms can be implemented either in hardware or software. In particular, typical image processing operations in digital cameras are dead-pixel correction, color interpolation, color conversion, data filtering, and data compression. Obviously, depending on the peculiarities of architecture and the noise properties of the sensor, different processing algorithms have to be developed and applied.

2.2 Noise Sources in Color CMOS Cameras

In CMOS imaging, there are two basic kinds of noise: read noise and fixed pattern noise (FPN). Read noise (also known as temporal noise) occurs randomly from time to time, is generated by several basic noise mechanisms of electronic components and looks to observers like the "snow" present on inactive TV channels. This noise can be minimized by careful electronic design. Under low-light and low-signal conditions where read noise exceeds photon noise data is read noise limited. Photon and dark current shot noise, *kTC* noise, and thermal noise are among the principal sources of read noise at the pixel. Photon shot noise follows the laws of phgsics and is generated by the random number of photons in the incident light sensed by a photodiode and follows a Poisson law. This noise level varies as function of the square root of the photon number. When photon noise exceeds system noise, data is photon shot noise limited.

FPN, on the other hand, does not change from frame to frame and is somewhat analogous to peering at scenes through a chain-link fence. This kind of noise, being one of the strongest degrading factors in CMOS imaging, is caused by mismatches in the device characteristics of the current reference array and of the pixel transistors. In modern sensors, analog processing techniques are used to reduce noise before the image signal leaves the sensor chip. For example, FPN can be significantly reduced using so-called correlated double sampling.

Obviously, different CMOS sensors have different noise properties. That is why at the first stage, it is necessary to analyze the noise characteristics of the sensor. It is worth-while to estimate the actual levels of temporal and fixed patter noise, their statistical properties, and the correlation properties between color channels. For this purpose, an appropriate methodology is to be developed using, for example, test images and statistical modelling. As a result, a model of noise or, at least, some noise characteristics of the output signal in the sensor are to be obtained. Then, such a model can be used for developing the noise removal algorithms.

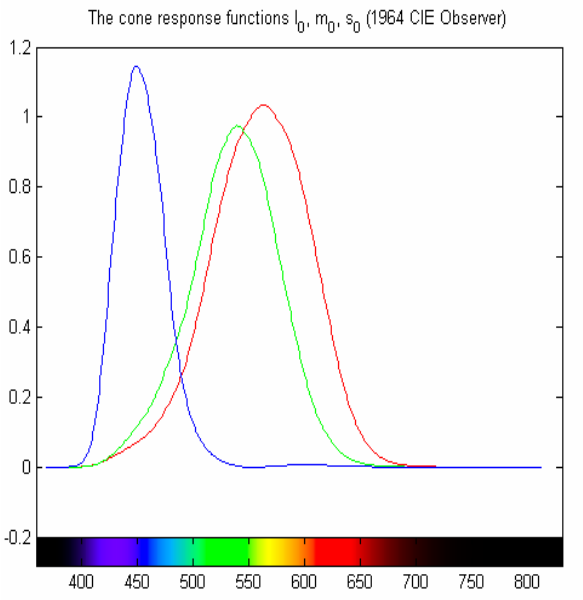

Fig. 2. RGB cone responses for LMS: long l_0 R, medium m_0 G, and short s_0 B cones.

2.3 Tri-stimulus for Representing Colors

Colors can be represented by three numbers – the so-called tri-stimulus, whether RGB or XYZ. This fact is a direct result of the physiology of human vision. Electromagnetic radiation whose wavelength is in the visible range (370 to 740 nanometers) is converted in the retinal cones into three signals, which correspond to the response of the three types of cones. This response is a function of wavelength and is described by the spectral sensitivity curves for the cones, as illustrated in Fig. 2.

Colored light can be represented as a spectral distribution, which plots power as a function of wavelength. In signal processing, plot spectra as a function of frequency is used, which is the inverse of wavelength. The cones convert this to three cone response values (*l, m, s*) that are the cone sensitivities in the long, medium, and short wavelength regions. So, colored light can be defined by integrating the product of the spectral sensitivity curves and the incoming spectrum. Two important principles follow from this process:

■ *Trichromacy*: all spectra can be reduced to precisely three values without loss of information with respect to the visual system – the tri-stimulus.

■ *Metamerism*: any spectra that create the same trichromatic response are indistinguishable. This means that two different spectra will look the same if they stimulate the same cone response.

In 1931, the Commission Internationale de l'Eclairage (CIE, or International Commission on Illumination) standardized a set of color-matching functions that form the basis for most color measurement instruments used today. They averaged experimental work from two independent sets of color-matching experiments performed on small visual fields (2 degrees), to create the 1931 standard observer, or the 2° observer. This standard observer statistically represents the average color-matching results for the human population having normal color vision. The 2-degree field is an important part of this specification. There is a second CIE standard observer, called the 10° observer, which was standardized in 1964, and should be used for fields larger than 4 degrees. Figure 6 shows the cone response functions for the 1964 standard observer.

The CIE recommendations that define CIE XYZ, and the standard functions needed to implement it, were first defined in 1931. They are the foundation for all modern color measurement and specification. Perception beyond tri-stimulus theory is an ongoing area of research, and progress over the past decade or so has provided some practical ways to model color perception beyond simple color matching. The cone response can be used to model the way the cones adjust to changes in illumination, a process called *adaptation*. The visual system adapts to both the brightness and the color of the ambient lighting, redefining "white." So, a transformation from the cone response (effectively RGB encoding signals) to a perceptual encoding (hue, lightness, and colorfulness) is achieved. The achromatic channel (A) is defined as the weighted sum of the cone response signals. The red-green opponent channel (R-G) is computed from the difference between the red (L) and green (M) channels, and the yellow-blue opponent channel is the difference between the yellow (L+M) and blue channels (S). Figure 11 shows a perceptual color space defined by these axes. Hue is defined as the angular dimension, saturation as the radial one.

Many perceptually organized color spaces exist. CIELAB and CIELUV are computationally derived from tri-stimulus values, plus the tri-stimulus values for a reference white. All perceptual models have a similar lightness axis and place hues in the same order around the hue circle, though the spacing of the hues varies. Most perceptual color systems are designed so that distance in the color space is proportional to perceptual distance. That is, they make it possible to compute how different two

colors appear. This is in contrast to tri-stimulus representations, which can only specify whether two colors match exactly.

A common feature of all perceptually organized spaces is a unique specification for white and black, in contrast to tri-stimulus values, where a wide range of values can appear white (depending on adaptation). In a physically defined color space, white is defined by the light illuminating the colored chips. In CIELAB and CIELUV, unique white is defined by dividing the tri-stimulus values of the stimulus by the tri-stimulus values of the reference white. For example, L*, which is the lightness axis for both spaces, is defined as a function of Y/Ywhite. It is tempting to convert tri-stimulus values to CIELAB or CIELUV, then use this specification to define colors in a different viewing environment, such as the display-to-print example previously mentioned. Perceptually, however, this is not as accurate a way to model adaptation as using LMS.

sCIELAB9 is an extension of CIELAB that uses spatial filtering in LMS to more accurately model the color of image pixels, which are both small and surrounded by pixels of various colors. Classic colorimetry assumes a 2-degree sample (about 5/8-inch across when viewed at a distance of 18 inches), viewed on a neutral background. Using sCIELAB rather than CIELAB for pixel colors gives a more accurate way to evaluate how similar two images appear. sCIELAB has been combined with the LMS projection algorithm previously described to create a tool for simulating on a display how colored images would appear to a person with color blindness (http://www.vischeck.com). The goal of the CIE color appearance models, CIECAM97s and CIECAM02,5 is to create models for color appearance that accurately predict perception, yet are computationally practical enough to apply to color reproduction problems such as gamut mapping and image quality assessment. These models take as input CIE XYZ for the stimulus and the reference white, plus parameters that describe the immediately surrounding color, the overall level of illumination, and to what degree the observer is adapted to the illumination. The outputs of these models are quantitative values for hue, lightness, brightness, chroma, saturation, and colorfulness, all of which are precisely defined as part of the modeling process. In applications, the goal is to preserve these quantities across different transformations of media and viewing environments. In general, perceptual and relative colorimetric spaces are best suited for photography because they aim to preserve the same visual appearance as the original. Two examples of such spaces are HVS and HSL (http://en.wikipedia.org/wiki/HSV_color_space). *HSL* stands for hue, saturation, lightness, while *HSV* stands for hue, saturation, value. They are illustrated in figures 3 and 4.

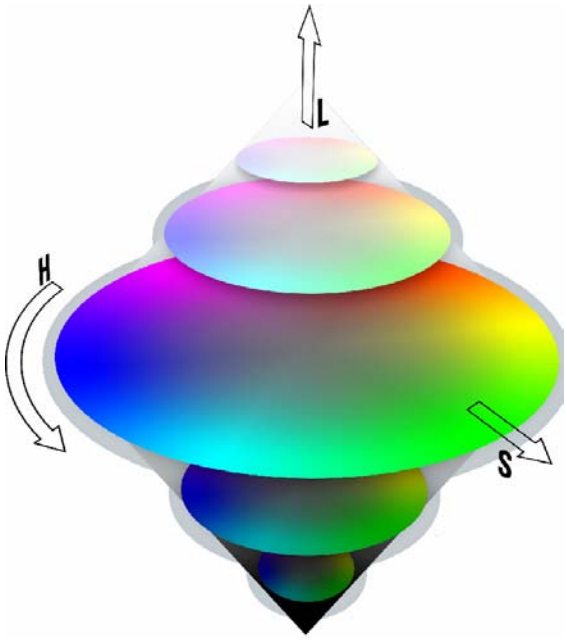

Fig. 3. HSL color space

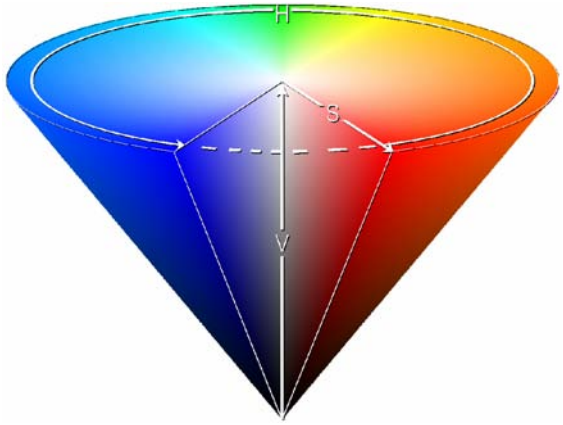

Fig. 4. HVS color space

2.2 Dynamic Range of CMOS Cameras

Dynamic range refers to intra-scene performance; that is, the ability to quantitatively detect very dim and very bright parts of a single image. Because the smallest measurable intensity varies between applications and experimental conditions, a definition for specifying dynamic range independent

of how the camera is used has been adopted. This is defined mathematically as the rate:

linear full well (electrons)/
read noise (electrons)

and is therefore a dimensionless number. The linear full well is a specific measure of pixel well capacity. The read noise (the noise associated with a single readout event) is usually minimized to yield the largest dynamic range possible.

As a general rule, camera cost increases with increasing dynamic range, so dynamic range requirements should be considered very carefully when selecting a camera.

3 Minimum Description Length

We start this section by defining the *complexity* of a given model *M* as

$$C_n(M) := \log \sum_{x^n \in \aleph^n} P\left(x^n \middle| \hat{\theta}(x^n) \right) \qquad (1)$$

where P is a probability distribution on X^n (P is not necessarily in M).

To get a first idea of why C_n is called model complexity, we note that the more sequences x^n with large $P\left(x^n \middle| \tilde{\theta}(x^n) \right)$, the larger $C_n(M)$. In other words, the more sequences exist that can be fit well by an element of M, the larger M's complexity is.

MDL tells us to pick the model $M^{(j)}$ maximizing the *normalized* maximum likelihood (NML) $P_{\mathrm{NML}}(D|M^{(j)})$, or, equivalently, minimizing

$$-\log P_{\mathrm{NML}}\left(D \middle| M^{(j)}\right) = -\log P\left(D \middle| \hat{\theta}^{(j)}(D) \right) + C_n\left(M^{(j)}\right) \qquad (2)$$

From a coding theoretic point of view, we associate with each $M^{(j)}$ a code with lengths $P_{\mathrm{NML}}\left(\bullet \middle| M^{(j)}\right)$, and we pick the model minimizing the code length of the data. The code length $-\log P_{\mathrm{NML}}\left(D \middle| M^{(j)}\right)$ has been called the *stochastic complexity of the data D relative to model $M^{(j)}$* [9], whereas $C_n(M^{(j)})$ is called the *parametric complexity* or *model cost* of $M^{(j)}$. We have already indicated that $C_n(M^{(j)})$ measures something like the 'complexity' of model $M^{(j)}$. On the other hand, $-\log P\left(D \middle| \hat{\theta}^{(j)}(D) \right)$ is minus the maximized log-likelihood of the data, so it measures something like (minus) fit or *error* – in the linear regression case it can be directly related to the mean squared error. Thus, (2) embodies a trade-off between lack of fit (measured by minus log-likelihood) and complexity (measured by $C_n(M^{(j)})$). The *confidence* in the decision is given by the codelength difference

$$\left| -\log P_{\mathrm{NML}}\left(D \middle| M^{(1)}\right) - \left[-\log P_{NML}\left(D \middle| M^{(2)}\right) \right] \right|. \qquad (3)$$

In general, $-\log P_{NML}\left(D \middle| M\right)$ can only be evaluated numerically; the exception is the case when M is from the Gaussian family. In many cases, even numerical evaluation is computationally problematic.

We will use MDL for modelling our data, in order to compare three models for camera characterization. Taking into consideration the polynomial transforms used in [7] and computational simplicity issues we considered the following models:

1. Polynomial model

$$\begin{aligned} M_1 = {} & a_0 + a_1 R + a_2 G + a_3 B + a_4 RG + \\ & a_5 GB + a_6 RB + a_7 R^2 + a_8 G^2 + a_9 B^2 + \\ & a_{10} R^2 GB + a_{11} RG^2 B + a_{12} RGB^2 + \varepsilon. \end{aligned} \qquad (4)$$

2. Fourier sine model (we considered camera response functions to be even)

$$\begin{aligned} M_2 = {} & a_0 + a_1 \sin R + a_2 \sin G + a_3 \sin B + \\ & a_4 \sin RG + a_5 \sin GB + a_6 \sin RB + \\ & a_7 \sin 2R + a_8 \sin 2G + a_9 \sin 2B + \\ & a_{10} 2RG + a_{11} \sin 2GB + \\ & a_{12} 2RB + \varepsilon. \end{aligned} \qquad (5)$$

3. Neural network model. We will not include this model in the current computation, but we will give the results of using this model in Section 4. We

just specify here that we start with a minimum size model, selectively add the needed neurons and prune the less fit neurons.

In order to estimate the optimal model by using the MDL principle we need to compute the stochastic complexity. The MDL principle states that the best model/model class among a collection of tentatively suggested ones is the one that gives the smallest stochastic complexity to the given data. In fact, by using the MDL principle we are looking for an optimal trade-off between the model complexity, which in our case is given by the number of coefficients and goodness-of-fit. The model complexity is increasing with the number of coefficients because the more coefficients M_1 or M_2 has, the more bits we need to describe it. Both models: polynomial model M_1 and sine Fourier series model M_2 will be used to compress the description of data points. The *RGB* values are regarded as given so we do not have to encode them.

When dealing with color images, which are multi-component images, a common problem is how to exploit the information present in various components. We have used a multi-dimensional Gaussian probability like in [6], to model the residual noise ε, se we considered the following density function:

$$P_{X,Y,Z}(\varepsilon, M) = \frac{q^d}{\left(\sqrt{2\pi}\right)^d \sqrt{\Sigma}} \exp\left[-\frac{\left(\{X,Y,Z\} - M\right)^2}{2\Sigma^2}\right] \quad (6)$$

where Σ represents the model of correlation between components and the amplitude of the noise.

Encoding the model *M* means to encode its parameters a_i for i = 0-12. This encoding will give us the complexity term. The overall optimum depends on both the degree of the polynomial and the precision with which the parameter values are encoded. Normally, we expect that the squared error to decrease as the order of the selected model is increasing, but the complexity of the model is increasing. We need to compute the maximum likelihood of data for the corresponding density function. The system formed by the following equations is obtained:

$$\frac{\partial \log P}{\partial a_i} = 0, \quad (7)$$

for i = 0,…,12. The NML density function is considered:

$$f(y^n, \gamma) = \frac{f(y^n, \gamma, \beta, \Sigma)}{\int_{Y(\tau_0, R)} f(z^n, \lambda, \beta, \Sigma) dz^n} \quad (8)$$

where $y = \{X, Y, Z\}$ and

$$Y(\Sigma_0, R) = \left\{z^n : \Sigma\left(z^n\right) \geq \Sigma_0, \beta'(z^n)\Sigma\beta(z^n) \leq R\right\} \quad (10)$$

The selection criterion is given by:

$$\min_{\gamma \in \Omega} \left\{ \begin{array}{l} (n-k)\ln\frac{n\Sigma}{n-k} + k\ln(nR) - \\ \ln\frac{n}{n-k} - (k+1)\ln k \end{array} \right\} \quad (11)$$

where *k* denotes the number of elements in γ and

$$R = \frac{1}{n}\beta'(s's)\beta \quad (12)$$

with s= $\{R,G,B\}$. The model that minimizes the above expression is the one that fits the data best. We will prefer the model class with the smallest stochastic complexity with respect to that model class.

4 Experimental Results

For the results presented in this paper we have used the Macbeth ColorChecker chart which contains a number of 24 patches. 160 training samples and 80 test samples were captured using this chart with 3.2 mega-pixels Nokia N93 camera phone. The 2048x1536 pixels color CMOS camera sensor of Nokia N93 comes equipped with a Carl Zeiss Vario-Tessar lens and 3X optical zoom. It has exposure compensation: +1 ~ -1EV at 0.5 step, focal length 4.5 mm (wide) /12.4 mm (tele) 34.25 - 94.1 mm(35mm equiv.), focus range 10m, macro focus distance 30 cm (macro at wide) and10 cm (macro at middle to tele), and a mechanical shutter with shutter speed of 1/2400~1/3 s. As suggested in [4],

we turned automatic white balance off, in order to obtain an effective camera characterization.

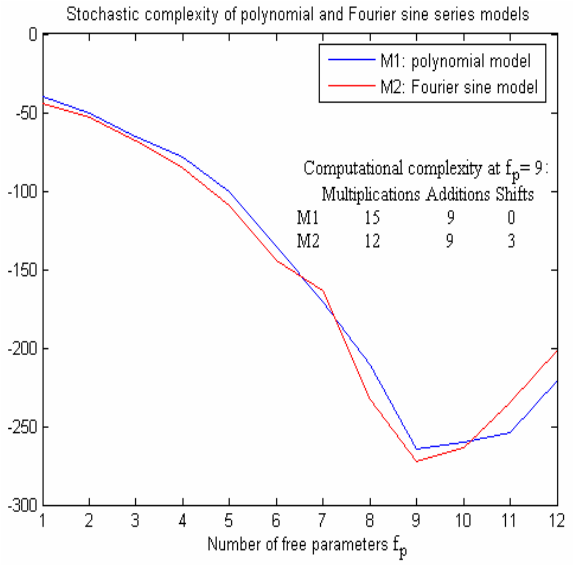

Fig. 5. Stochastic complexity and computational complexity of polynomial and Fourier sine series models

The training samples were used to train the neural network and to determine the stochastic complexity using the MDL formalism for polynomial and Fourier sine models.

i	7	8	9	10	11
M_1	-191.1	-244.3	-295.3	-280.1	-275.5
M_2	-175.3	-252.6	-303.8	-293.1	-262.1

Table 1. Stochastic complexity of M_1 and M_2.

In Table 1 the results for the two models M_1 and M_2 are presented. On the first line the number of free parameters a_i, with i ranging from 7 to 11, is given. The results for values smaller than 7 or bigger than 11 are increasing, so we consider them not to be of interest. For space economy we decided not to display them in the table. All computed values are illustrated graphically in Figure 5. On the second line the results for the polynomial model M_1, and on the third line the ones for the Fourier sine model M_2, are given. From these results we conclude that for the both models the best model order is 9.

The Fourier series model M_2 has the smallest stochastic complexity, so it is the best one for the given data. For this model order, the polynomial model M_1 has the computational complexity of 15 multiplications and 9 additions, while the Fourier sine model M_2 has the computational complexity of 12 multiplications, 9 additions and 3 shifts.

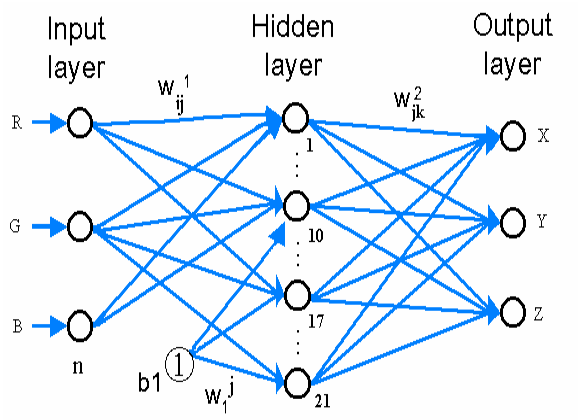

Fig. 6. Obtained ANN

For the neural network model, we started with 3 input and output units, and 1 hidden unit. The neural network was trained by adding units in the hidden layer using a procedure with a MDL stopping criterion similar with the one presented in [4]. The resulted neural network contained 21 hidden units, and is illustrated in Fig. 6. The presented results are average values from training the neural network models 10 times.

Model	M_1	M_2	ANN
Median CIELAB error	1.98	1.12	1.24
Maximum CIELAB error	30.4	25.9	34.1

Table 2. Performance of tested models.

The obtained models were then tested using the test samples. The color errors between measured and estimated tri-stimulus values were computed using the CIELAB color difference formula. The maximum and median CIELAB errors for the used 3 models are given in Table 2. We note that better performances are obtained by the models with a stronger nonlinear character.

4 Conclusion

In this paper, the MDL formalism has been used to study the low-end digital camera characterization of a Nokia imaging phone. Three different models have been considered: polynomial transforms, Fourier sine transforms, and neural networks. Better performances were obtained for the models with higher nonlinear characteristics. The abilities of camera characterization models based on Fourier sine and neural networks are slightly similar and better than those of the polynomial model.

References:

[1] M.C. Stone, "Representing colors as three numbers [color graphics]," *IEEE Computer Graphics and Applications*, Vl. 25, No. 4, July-August 2005, pp. 78-85.

[2] Red Herring, "Photo phones hurting cameras," *http://www.redherring.com/*, August 2005.

[3] F. Galland, N. Bertaux, and P. Refregier, "Minimum description length synthetic aperture radar image segmentation," *IEEE Transactions on Image Processing*, vol. 12, no. 9, pp. 995–1006, September 2003.

[4] S. Pateux, "Spatial segmentation of color images according to the mdl formalism," *Proceedings of the International Conference on Image Processing ICIP*, vol. 2, pp. 554–557, September 2000.

[5] V. Cheung, S. Westland, D. Connah, and C. Ripamonti, "A comparative study of the characterisation of colour cameras by means of neural networks and polynomial transforms," *Coloration Technology*, vol. 120, no. 1, pp. 19–25, 2004.

[6] Yu Ning Lai and Shiu Yin Yuen, "Successive-least-squares error algorithm on minimum description length neural networks for time series prediction," *Proceedings of the 17th International Conference on Pattern Recognition ICPR*, vol. 4, pp. 609–612, August 2004.

[7] T.L.V. Cheung and S. Westland, "Colour camera characterisation using artificial neural networks," *Proceedings of the 10th Color Imaging Conference*, pp. 117–120, 2002.

[8] Hong Guowei, Han Bing, and M.R. Luo, "Colorimetric characterisation of low-end digital camera and its application for on-screen texture visualisation," *Proceedings of the International Conference on Image Processing ICIP 2000*, vol. 1, pp. 741–744, September 2000.

[9] J. Rissanen, "Strong optimality of the normalized ml models as universal codes and information in data," *IEEE Transactions on Information Theory*, vol. 47, no. 5, pp. 1712–1717, June 2001.

[10] E. R. Fossum, "CMOS image sensors: electronic camera-on-a-chip," *IEEE Transactions on Electron Devices*, vol. 44, pp. 1689 -1698, 1997.

[11] Y. T. Tsai, H. Wei-Geng, T. Shinn-Yih, and C. Shih-Liang, "Optimized image processing algorithms for a single sensor camera," in *Proc. of the IEEE Pacific Rim Conference on Communications, Computers and Signal Processing IPRCCSP, 1997*, vol. 2, pp. 1010-1013, 1997.

[12] Y. T. Tsai, "Color image compression for single-chip cameras," *IEEE Transactions on Electron Devices*, vol. 38, pp. 1226-1232, 1991.

[13] S. K. Mendis, S. E. Kemeny, R. C. Gee, B. Pain, C. O. Staller, K. Quiesup, and E. R. Fossum, "CMOS active pixel image sensors for highly integrated imaging systems," *IEEE Journal of Solid-State Circuits*, vol. 32, pp. 187 -197, 1997.

[14] A. J. Blanksby, M. J. Loinaz, D. A. Inglis, and B. D. Ackland, "Noise performance of a color CMOS photogate image sensor," in *Technical Digest. of IEEE International Electron Devices Meeting,* vol. 2, pp. 205-208, 1997.

[15] D. X. Yang, H. Min, B. A. Fowler, A. E. Gamal, M. Beiley, and K. Cham, "Test structures for characterization and comparative analysis of CMOS image sensors," in *Advanced Focal Plane Arrays and Electronic Cameras. Proc. of SPIE.* (T. M. Bernard, ed.), vol. 2950, pp. 8-17, 1997.

[16] Kobus Barnard & Brian Funt. "Camera Characterization for Color Research", *Color Research and Application*, 2001. http://www.CS.Berkeley.EDU/~kobus/research/publications/camera_characterization/index.html.

[17] Eyal de Lara, K. Farkas, "New Products", *IEEE Pervasive Computing*, vol. 5, no. 1, pp. 12 – 15, Jan.-March 2006.

[18] X.-S. Hua, S. Li, H.-J. Zhang, "Camera notes", *IEEE International Conference on Multimedia and Expo ICME 2005*, 6-8 July 2005.

[19] Poorvi Vora & Joyce Farrell. "Digital Color Cameras - 1 - Response Models". *Hewlett-Packard Laboratory*, Technical Report.

[20] Poorvi Vora & Joyce Farrell. "Digital Color Cameras - 2 - Spectral Models". *Hewlett-Packard Laboratory*, Technical Report.
[21] G. E. Healey and R. Kondepudy, "Radiometric CCD camera calibration and noise estimation," *IEEE Trans. Image Process.*, vol. 16, no. 3, pp. 267–276, Mar. 1994.